DOI: 10.2478/v10077-008-0021-6

M. Szkodo
Gdansk University of Technology, Department of Materials Science and Engineering, Gdansk, Poland

CAVITATION EROSION OF X5CrNi18-10 AUSTENITIC STAINLESS STEEL ALLOYED WITH TiC

ABSTRACT

This work presents investigations of cavitation resistance of X5CrNi18-10 austenitic stainless steel after alloying its surface by CO_2 laser beam. Laser beam machining was performed in two variants. In the first case, surface layer was enriched with TiC in amount of 1.55 % wt. and in the second one in amount of 3.97 % wt. The obtained results revealed that content of 3.97 % wt. TiC caused an increase of plastic deformations resistance of surface under the cavitation loading and simultaneous increase in embrittlement of alloyed layer.

Key words: *cavitation, erosion, laser beam processing, austenitic stainless steel*

INTRODUCTION

The cavitation phenomenon composes of in nucleation and growth vapor bubbles in liquids followed by violent collapse. The repeated cycle of cavitation near the surface of materials locally induces high tensile and compressive stress cycles which lead to erosion of the surface as a portion of the impact energy is transformed into plastic deformation and fracture. Owing to the special features of attack, which include randomness, impulsiveness, localization of stress and repetitiveness, cavitation erosion is a unique type of material degradation which has to be independently studied and assessed. The failure of pipelines, pumps, water turbine blades and other hydraulic sets can often be attributed to cavitation erosion.

Austenitic stainless steel is widely used in hydraulic machinery and in liquid-handling systems mainly because of its excellent corrosion properties, good machinability and relatively low cost. However, due to its low hardness, austenitic stainless steels might not be adequate in resisting cavitation attack in harsh environments. As cavitation erosion is a surface degradation process, one route to improve the cavitation erosion resistance of a material is to employ surface modification. In this respect, laser surface modification is particularly suitable as the modified surface layer is tightly bonded to the substrate by fusion bonding and the heat-affected zone (HAZ) is small, in addition to the attainment of desirable microstructural features such as fine grain size and non-equilibrium alloy composition [1,2]. In these studies, the increase in cavitation erosion

resistance is mainly attributed to an increase of hardness arising from the presence of hard TiC phase.

EXPERIMENTAL PROCEDURES

Two round test specimens (diameter 30 mm and height 8 mm) were made of X5CrNi18-10 steel. Next powder of TiC was mixed with natrium water glass and the layers were placed by pasting on the samples surfaces. Thickness of the pasted layers and the parameters of laser beam processing were chosen to obtain assumed concentration of TiC in modified surface layer (1.55 and 3.97 wt.% of TiC). Subsequent laser melting of the paste with surface layer of the processed steel gave an alloyed samples. Continuous work CO_2 laser TRIUMPH TLF 6000 was used as a power source. The beam power on the samples surfaces was attenuated of 3% due to multiple reflections along optical trail. During the experimental runs the samples of X5CrNi18-10 steels were moved across the laser beam along single 0.30 cm wide path (Fig. 1).

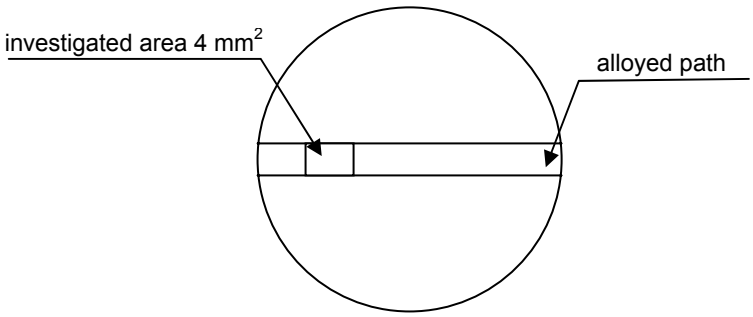

Fig. 1. Scheme of the processed surface of the investigated sample

Argon of purity 99.998 % was used as a shielding gas. An example of chemical composition of the investigated sample detected by electron dispersive spectroscopy is presented in Fig. 2.

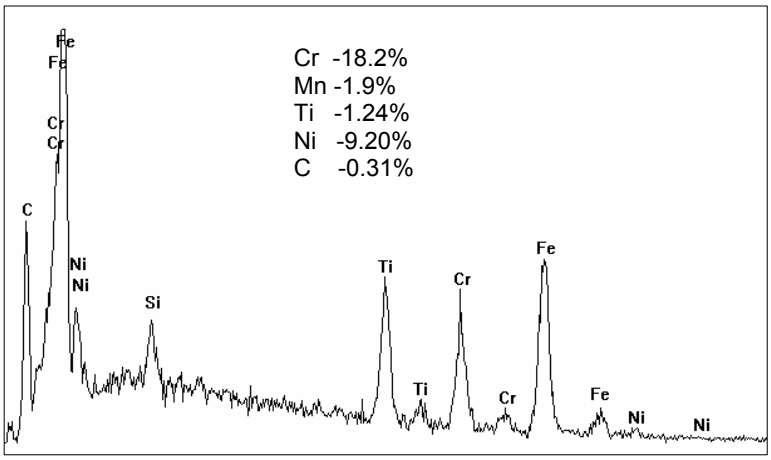

Fig. 2. SEM-EDS microanalysis pattern obtained for sample containing 1.55% wt. of TiC

Before setting the processed samples into rotating disk, the grinding and polishing of their surfaces was performed. Next the processed samples were subjected to cavitation loading at the rotating disk facility [3] in the Institute of the Fluid-Flow Machinery in Gdańsk. The cavitation was generated there by means of cylinders situated on the disk surface on the circle which diameter equalled 300 mm (see Fig. 3). The specimens were inlaid in the disk, downstream of the cavitator. Their rotation speed stand for 3000 r.p.m. Resulting mean gauge

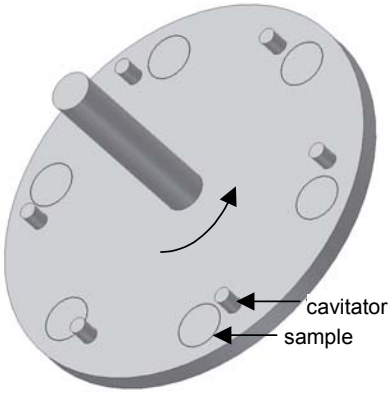

Fig. 3. Scheme of the rotating disk

pressure was 155 kPa. The water, which temperature equalled 20 °C, was used as an active medium.

The tests were performed in runs 2-5 min long following one after another, lasting 52.5 minutes in total. The duration of each run was lower than the time needed to achieve the steady state cavitation intensity. After each run the plastic deformation on the processed surfaces caused by cavitation loading was investigated. The procedures of calculation of resistance of processed surface to plastic deformation under cavitation loading using an image analysis of monochromatic picture of eroded surface were elaborated. Relative plastic deformation was defined as a black area fraction in the binary image of eroded surface. Binary image was obtained by binarisation of monochromatic picture with threshold 150. It means that every pixel of monochromatic picture was changed to black if its brightness on monochromatic picture was lower than 150. In the opposite case, the pixel was changed to white (monochromatic picture i.e. eight-bit picture has $2^8 = 256$ levels of gray). Cavitation properties of laser processed materials were calculated on the surface of 4 mm^2.

RESULTS AND DISCUSSION

The series of cavitation erosion curves (i.e. time variations of relative plastic deformation) are presented in Fig. 4. By examining of this figure can notice fast increase plastic deformation of eroded surface for not processed sample during first stage of cavitation erosion in comparison with alloyed areas. After 2 minutes of cavitation loading on the surface of this sample the increment of plastic deformation was almost the same as for sample alloyed with 3.97% TiC and lower than for second

one. It can be explained by fact that austenitic microstructure of chromium-nickel 18-10 stainless steel is much more susceptible to work hardening then austenite strengthened by presence of TiC carbides, so the hardness of the surface of not processed sample is enhanced due to cavitation loading and then the generation of the pits is restrained.
Cavitation energy emitted during bubble collapse is changed to work of plastic (W_{pl}) and elastic deformation of surface (W_{el}) (no taking into account of thermal and other effects accompanying of cavitation). Energy of cavitation cloud is constant on the investigated surface i.e. $W_{pl}+W_{el}$ = const but $W_{pl} \neq$ const and it can decrease, for example, due to work hardening or stress or strain induced phase transformations. W_{pl} can be calculated as the areas under the curves presented in the Fig. 4.

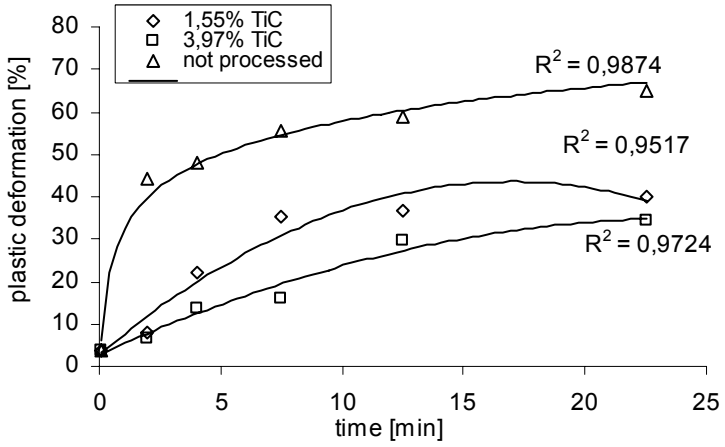

Fig. 4. Plastic deformation vs. time of cavitation erosion during incubation period

Figure 5 presents relative work of plastic deformation W_{pl} for investigated samples calculated for time interval 0-20 min. Observing Fig. 5 one can notice that relative work of plastic deformation W_{pl} for not processed sample is almost three times higher than for sample enriched with TiC carbides in amount of 3.97% wt. In [4-6] were reported values susceptibility of chromium nickel stainless steel to phase transformation due to cavitation

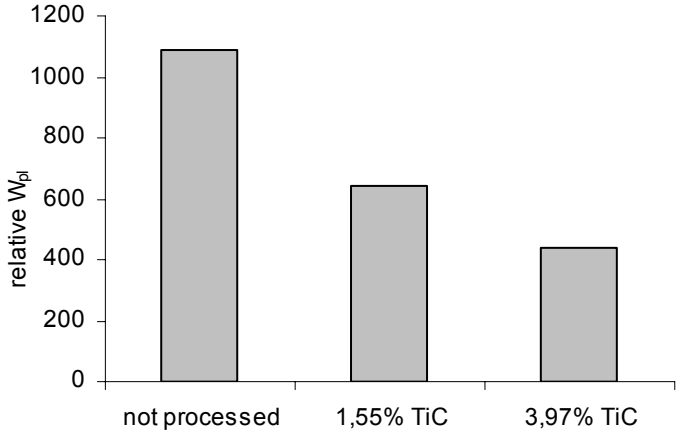

Fig. 5. Relative work of plastic deformation W_{pl} for investigated samples

loading. Part of energy emitted during bubble collapse can be changed then to phase transformation. Results of hardness investigations (Fig. 6) indicate that X5CrNi18-10 steel strengthened by TiC precipitations is not susceptible to work hardening due to cavitation loading. It is because part of TiC dissolved in austenite during laser alloying

and changed microstructure of processed steel. After laser beam alloying microstructure composed of austenite, δ-ferrite and TiC precipitations (Fig. 7a). Mills and Knutsen reported [7] that the presence of δ-ferrite adversely affects the erosion resistance, because material is more likely to be lost from δ-ferrite grains than from austenite grains during the early part of cavitation erosion. Less strain can be accommodated by the δ-ferrite due to its much lower work-hardening capacity, with the result that a more brittle failure mode occurs in this region (see Fig. 8a).
Fig. 7 shows the change of ferrite volume content in the surface of sample alloyed with 1.55% TiC during cavitation erosion process. It can be found that ferrite volume content decreases as cavitation erosion time increases. When the surface is impacted by high speed microjet formed in the cavitating liquid, the material deforms at high strain rate [8]. Such deformation causes easier ferrite fracture and removal from the surface than that of austenite because the face-centered cubic (fcc) structure has low sensitivity to the strain rate [9]. So it can be found that ferrite is more prone to removal from the eroded surface than austenite.

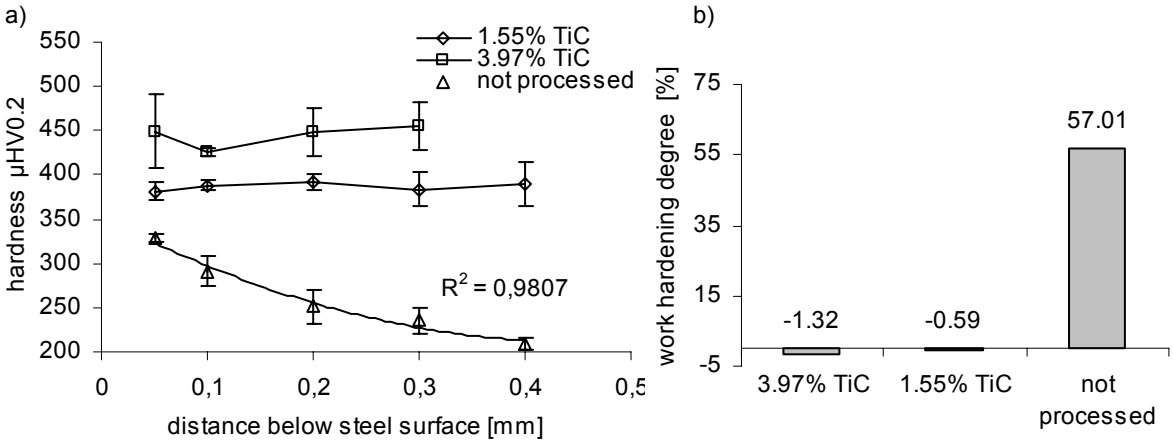

Fig. 6. Microhardness profiles after cavitation test – Fig. a) and work hardening degree – Fig. b)

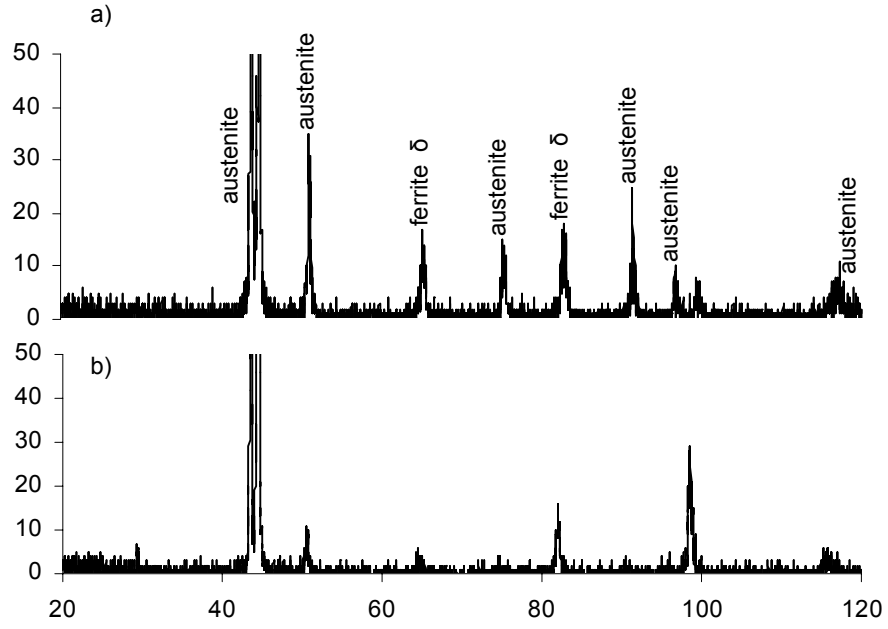

Fig. 7. The X-ray diffraction pattern of TiC alloyed path – Fig. a) and the same area after 52.5 min of cavitation loading – Fig. b)

On the other hand, C element dissolved in austenite during TiC alloying can stabilize austenite and improve the deformation strengthening ability of the processed steel, so martensitic transformation is restrained (Fig.7b). Therefore, there must exist other mechanisms of absorbing or dissipating the energy. Maximal standard deviation of hardness for sample enriched with 3.97% TiC occurs on the sample surface and for sample alloyed to content of 1.55% TiC 0.4 mm below steel surface. For lower content of TiC, austenite with TiC precipitations is surrounded by δ-ferrite of needle shape. The cracks in this sample are nearly parallel to each other and nearly parallel to the eroded surface (Fig. 8b). They start from top of needle of δ-ferrite and propagate across strengthened austenite. The case of sample enriched with 3.97% TiC is different. In this sample the erosion attack is initiated at the carbide/matrix interface and cracks start to propagate from carbides along the grain boundary.

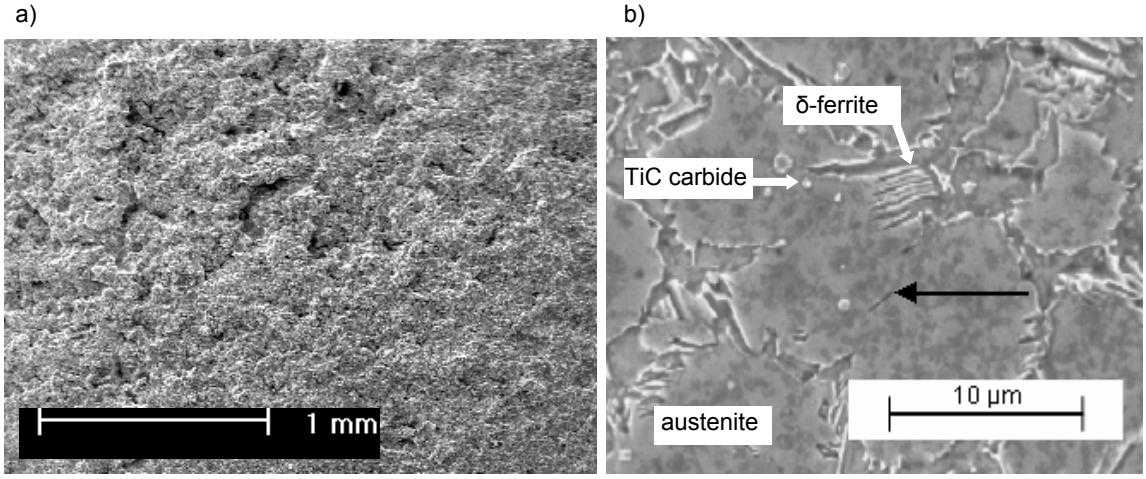

Fig. 8. Surface of the sample enriched with 1.55% of TiC after 52.5 min of cavitation loading – Fig. a) and cross-section the same sample, with visible crack (depicted by black arrow) developing across the austenite grain – Fig. b)

CONCLUSION

1. There is no martensitic transformation in the eroded surface of processed steel during cavitation erosion process. Ferrite content in processed steel decreases due to cavitation loading.
2. There is no susceptibility to work-hardening of TiC alloyed steel. Cracks initiating in the eroded austenite of 1.55% TiC steel propagate nearly parallelly rather than normally to the surface, and for 3.97% TiC cracks start to propagate from carbides along the grain boundary.

REFERENCES

1. Fellowes F.C.J., Steen W.M., Rickerby D.S., Matthews A.: (Ed.) Laser Surface Treatment, (1991), Advanced Surface Coatings, Blackie, USA. pp. 244-277.

2. Ready J.F., Farson D.F.: LIA Handbook of Laser Materials Processing, first ed. (2001), LIA Magnolia Publishing, Orlando. pp. 263–297.
3. Steller K., Krzysztofowicz T., Reyman Z.: Effects of cavitation on materials in field and laboratory conditions. ASTM Special Tech. Pub. 567 (1974), pp.152.
4. Szkodo M.: Cavitation erosion behaviour of 18/8 stainless steel after its laser alloying of manganese. Solid State Phenomena 113 (2006), pp.513-516.
5. Heathcock C.J., Protheroe B.E., Ball A.: Cavitation of stainless steels. Wear 81 (1982), pp. 311-327.
6. Fu W.T., Yang Y.B., Jing T.F., Zheng Y.Z., Yao M.: The resistance to cavitation erosion of Cr–Mn–N stainless steels. J. Mater. Sci. Perform. 7 (1998), pp. 801-804.
7. Mills D.J., Knutsen R.D.: An investigation of the tribological behaviour of a high-nitrogen Cr-Mn austenitic stainless steel. Wear 215 (1998), pp. 83-90.
8. Karimi A., Martin J.L.: Cavitation erosion of metals. Int. Metals Rev. 31 (1986), pp.1-35.
9. Al-Hashem A., Caceres P.G., Bdullah A.A., Shalaby H.M.: Cavitation corrosion of duplex stainless steel in seawater. Corrosion 53(2) (1997), pp. 103-113.